HAL
open science

Characterization of B-H agostic compounds involved in the dehydrogenation of amine-boranes by group 4 metallocenes

Jingwen Zhu, Emilie-Laure Zins, Mohammad Esmaïl Alikhani

To cite this version:

Jingwen Zhu, Emilie-Laure Zins, Mohammad Esmaïl Alikhani. Characterization of B-H agostic compounds involved in the dehydrogenation of amine-boranes by group 4 metallocenes. Journal of Molecular Modeling, 2016, 22 (12), pp.294. 10.1007/s00894-016-3165-z . hal-01497705

HAL Id: hal-01497705

https://hal.sorbonne-universite.fr/hal-01497705v1

Submitted on 29 Mar 2017

HAL is a multi-disciplinary open access archive for the deposit and dissemination of scientific research documents, whether they are published or not. The documents may come from teaching and research institutions in France or abroad, or from public or private research centers.

L'archive ouverte pluridisciplinaire **HAL**, est destinée au dépôt et à la diffusion de documents scientifiques de niveau recherche, publiés ou non, émanant des établissements d'enseignement et de recherche français ou étrangers, des laboratoires publics ou privés.

Characterization of B-H agostic compounds involved in the dehydrogenation of amine-boranes by group 4 metallocenes

Jingwen Zhu,[a,b] Emilie-Laure Zins, [a,b] Mohammad Esmaïl Alikhani [a,b]

a: Sorbonne Universités, UPMC Univ. Paris 06, MONARIS, UMR 8233, Université Pierre et Marie Curie, 4 Place Jussieu, case courrier 49, F-75252 Paris Cedex 05, France

b : CNRS, MONARIS, UMR 8233, Université Pierre et Marie Curie, 4 Place Jussieu, case courrier 49, F-75252 Paris Cedex 05, France

Abstract

For over a decade, amine-borane is considered as potential chemical hydrogen vector in the context of a search for cleaner energy sources. When catalyzed by organometallic complexes, the reaction mechanisms currently considered involve the formation of β-BH agostic intermediates. A thorough understanding of these intermediates may constitute a crucial step toward the identification of ideal catalysts. Topological approaches such as QTAIM and ELF revealed to be particularly suitable for the description of β-agostic interactions. When studying model catalysts, accurate theoretical calculations may be carried out. However, for a comparison with experimental data, calculations should also be carried out on large organo-metallic species, often including transition metals belonging to the second or the third row. In such a case, DFT methods are particularly attractive. Unfortunately, triple-ζ all electrons basis sets are not easily available for heavy transition metal elements. Thus, a subtle balance should be reached between the affordable level of calculations and the required accuracy of the electronic description of the systems. Herein we propose the use of B3LYP functional in combination with the LanL2DZ pseudopotential for the metal atom and 6-311++G(2d,2p) basis set for the other atoms, followed by a single point using the DKH2 relativistic Hamiltonian in combination with the B3LYP/DZP-DKH level, as a "minimum level of theory" leading to a consistent topological description of the interaction within the ELF and QTAIM framework, in the context of isolated (gas-phase) group 4 metallocene catalysts.

Introduction

Numerous experimental and theoretical studies have demonstrated the capability of organometallic compounds in catalyzing the dehydrogenation of amine-boranes.[1-5] Of particular importance for actual applications as energy carriers is the detailed reaction mechanism.[6] Indeed, viable alternative proposal for energy source should satisfy the requirements for sustainable development and green chemistry. As such, care should be taken in step economy and redox economy, which cannot be done without an in-depth understanding of the detailed reaction mechanisms. Based on theoretical as well as experimental investigations, reaction mechanisms were proposed to explain the catalytic cycles leading to the generation of molecular hydrogen from amine boranes. The exact role of the metallic centre M on these reaction mechanisms is still the topic of numerous studies.[7] At the molecular scale, different non-covalent interactions are involved in these dehydrocoupling reactions: the formation of a 3 centre - 2 electrons (3C/2e) intermediate, and Kubas' complexes.[1-8] The former species may play a critical role in the reaction, because of the activation of the σ(B-H) bond.

The term "agostic"[9] will be used throughout the present article to describe 3C/2e interaction between a σ(B-H) bond and a metal atom in an organometallic complex. A unique and unequivocal definition of the term agostic would deserve consideration.[10] First proposed by Brookhart and Green in 1983, the term was specifically introduced to describe a 3C/2e interaction involving a H-C bond.[11, 12] Should the chemical nature of the σ bond involved in the interaction, be considered as a criterion in the use of the "agostic" term? This question was discussed, as was the definition of this interaction. Phenomenological 3C/2e as well as causal (i.e. based on reactivity properties) criteria were applied to use the "agostic" term. Since the phenomenological 3C/2e criterion is used (even tacitly) in almost all the articles dealing with the organometallic-catalyzed dehydrocoupling of amine borane, we will use the term "agostic intermediate" to refer to as the activated species involving a 3C/2e interaction. A thorough understanding of the parameters influencing this interaction may help in choosing either the best catalysts with a given amine-borane compound, or conversely the best N-B (or P-B) containing precursor with a given catalyst, for the generation of molecular hydrogen. The first step toward such an understanding is methodological: a step by step study to analyze the effects of the nature of (1) substituents beared by the ligand, (2) the ligand (amine- versus phosphine-boranes), (3) the metallic centre, and (4) the magnetic properties of the metallic centre, is a needed prerequisite prior to a more systematic computational study. We are convinced that the electron localization function (ELF)[13] and the quantum theory of atoms in molecules (QTAIM)[14,15] topological approaches constitute appropriate tools for such a methodological study.

An appropriate electronic and geometric description of the organometallic complex is a prerequisite to any *a posteriori* topological characterization of the agostic interaction. First discussed by Streuber and Grunenberg in the case of titanium compounds,[16] and by Etienne et al. in the case of niobium compounds,[17] this point is particularly challenging for three main reasons: i) due to the size of the systems, ab initio methods can hardly be carried out in the context of a comparative study; ii) it is a non-covalent intramolecular interaction; and iii) the electronic properties of the d-bloc atoms should be accurately described. Comparison between theoretical studies based on the density functional theory (DFT) and experimental structures definitely suggests that agostic interactions can be described by DFT functionals.[18] Recently, different approaches were implemented in quantum chemistry programs to allow the treatment of dispersion forces in DFT calculations. Such dispersion forces are of fundamental importance in the case of van der Waals interactions. They also may play a prominent role in the case of hydrogen bondings. Among other methods, the D3 empirical correction of Grimme with Becke and Johnson damping was revealed to be particularly adapted to describe intramolecular hydrogen bondings.[19] Would such correction affect the description of agostic interactions, either from a geometric or from a topological point of view?

As far as the electronic description of the metallic centre is concerned, all-electron basis sets can be practically used only in the case of the first-row transition metal elements. For heavier elements, pseudopotentials should be chosen. The further use of relativistic Hamiltonian is needed for an accurate description of topological properties of organometallic compounds.[20,21,22] Herein is proposed an estimation of the "minimum level of theory" leading to accurate enough topological description of β-agostic interactions within the framework of the DFT. The accuracy of the levels of theory was evaluated on a model system in a three-step approach:

- first, geometric parameters were used to characterize the ability of the level of theory to describe the agostic interaction ,
- then, the existence of a trisynaptic basin for the hydrogen atom involved in the agostic interaction was checked using the ELF topological method,
- finally, the ρ, $\nabla^2\rho$, ε and H QTAIM descriptors on the BCP of the agostic bond obtained from DFT calculations carried out at different levels of theory were compared

The influence of the DFT level of theory on the accuracy of the geometric and topological description of the agostic interaction was thus evaluated. A suitable level of theory was then selected for an analysis of a large, representative, set of agostic compounds.

Computational details

A set of nine group 4 metallocenes for which experimental data were reported in the literature, was chosen for this study: $Cp_2TiNH_2BH_3$,[23] $Cp_2ZrHNH_2BH_3$ and its isomer,[24] $Cp_2TiNMe_2BH_3$,[25] $Cp_2ZrHNMe_2BH_3$,[25] $Cp_2TiPPh_2BH_3$,[25] and $Cp_2ZrPPh_2BH_3$.[25]

All the geometry optimizations were carried out using the Gaussian09 software.[26] The effects of several exchange-correlation functionals and basis sets (including the treatment of relativistic effects) on the geometric and electronic (topological) description of the agostic interaction in the metallocenes were evaluated. This calibration step was carried out on the titanocene aminoborane (compound 1) for which experimental data are available.[23] The Minnesota[27] and range-separated hybrid functionals,[28] dedicated to the study of weak interactions, were considered for the present methodological study.[29,30,31] Additionally, the effect of the dispersion-correction within the framework of the Becke-Johnson damping function[32,33] was evaluated in the present work.[34,35] The following functionals were considered in the present work:

- The local functional M06-L [36] designed for taken into account the exchange-correlation energy ,
- The GGA BP86 functional,[37] alone and with the D3 empirical correction of Grimme with Becke and Johnson damping,
- The Meta-GGA TPSSTPSS [38] functional, alone and with the D3 empirical correction of Grimme with Becke and Johnson damping,
- The hybrid B3LYP,[39,40] B3PW91, PBE1PBE,[41, 42,43] M06 and TPSSh[44] functionals, alone and with the D3 empirical correction of Grimme with Becke and Johnson damping ,
- The LC-ω-PBE range separated RSH functional,[45,46,47] alone and with the D3 empirical correction of Grimme with Becke and Johnson damping. All the calculations were carried out with the default value of ω in the Gaussian09 software (ω = 0.4 a.u.$^{-1}$).

Complementarily, the influence of the basis set was studied. In the case of the titanocene compounds, Pople triple ζ basis sets can be used for all the elements, including the transition metal atom. This is not the case for the zirconocene and hafnocene compounds. For these latter cases, the use of pseudopotentials is needed. To determine how these pseudopotentials will affect the description of the agostic interactions, model Ti^{+III}(1) and Ti^{+IV}(1) species were studied using the following basis sets:

- The Pople triple ζ 6-311++G(2d,2p) and 6-311++G(3df,3pd) basis sets,
- The Def2-TZVP, Def2-TZVPP and def2-QZVPPD basis sets,
- The Pople triple ζ 6-311++G(2d,2p) basis set for the main-element atoms in combination with the SDD pseudopotential for the titanium. This basis set will be further referred to as 6-311++G(2d,2p)+SDD,
- The Pople triple ζ 6-311++G(2d,2p) basis set for the main-element atoms in combination with the relativistic LanL2DZ pseudopotential for the titanium. This basis set will be further referred to as 6-311++G(2d,2p)+LanL2DZ,
- The DZP [48,49,50] and TZP[51,52,53] basis sets,
- The relativistic DZP-DKH[54,55,56] and TZP-DKH[56, 57] basis sets, in combination with the Douglas-Kroll-Hess Hamiltonian, in the context of relativistic calculations,[58]
- The relativisic RESC approach, in combination with the DZP-DKH basis set.

The nature and the strength of the interactions were further characterized with two topological approaches: the electron localization function (ELF)[13] and the Quantum Theory of Atoms in Molecules (QTAIM).[14,15] The ELF streamlines and specifies the chemical bond, in line with the concepts initially introduced by Lewis.[59,60] This interpretative tool allows for a partition of space in terms of basins. The number of electrons involved in each basin (i.e. the basin's population), as well as other properties, can easily be obtained by integrating of the property density over the basin volume. The ELF signature of a X-H agostic interaction consists in a protonated basin containing approximately 2 electrons from the X, H and M atoms. Such basins are described as "trisynaptic". The ELF identification of a trisynaptic basin containing approximately two electrons constitutes a necessary and needed proof to the existence of a 3C/2e interaction. In the QTAIM framework, proposed and thoroughly developed by Bader and co-workers, the identification of a bond critical point (BCP) as well as a bond path (BP) between two atoms proves that the two atoms are chemically bonded. In such a case, the chemical bond can be further (quantitatively) characterized by means of the electron density (ρ), the Laplacian of ρ ($\nabla^2\rho$), the ellipticity (ε), and the total energy density (H) on the BCP. Other specific (local) descriptors were also introduced in the context of agostic interactions by Joubert et al.[61, 62, 63]. Using the above-mentioned values, the strength of agostic interactions can be accurately evaluated as soon as the interaction is characterized by a BCP. This is generally the case for β agostic interactions, but not necessarily for α agostic interactions. Since the present article focuses on β agostic interactions, the QTAIM tool will be used to estimate the strength of the interaction between the metallic centre and the B-H bond.

All the geometry optimizations and the generation of the *wfn* files were carried out with the Gaussian 09 Rev D.01 software. The *wfn* files were further used for the topological analysis. The ELF and QTAIM calculations have been done using the TopMod [64] and AIMAll [65] softwares, respectively. The ELF analyses were carried out using the "fine" grid. As far as the QTAIM calculations are concerned, we should point out the fact that the energy densities are evaluated from the Kohn-Sham first reduced density matrix.

Results and discussion

The $Cp_2TiNH_2BH_3$ compound, for which experimental data are available, was chosen to evaluate the accuracy of the description of the agostic interaction calculated at the different levels of theory. [23]

1. Geometric considerations

Different representative geometric parameters were compared with experimental data. Deviations between experimental and theoretical d_{X-Y} distance between X and Y atoms were calculated as follows:

$$\delta d_{X-Y} = \frac{d_{X-Y}^{calc.} - d_{X-Y}^{exp.}}{d_{X-Y}^{exp.}} \times 100$$

where $d_{X-Y}^{exp.}$ (respectively $d_{X-Y}^{calc.}$) represents the experimental (respectively calculated) distance.

Similarly, deviations between experimental and theoretical $X\widehat{-Y-}Z$ angle between X, Y and Z atoms were calculated as follows:

$$\delta_{X-Y-Z} = \frac{X\widehat{-Y-}Z^{calc.} - X\widehat{-Y-}Z^{exp.}}{X\widehat{-Y-}Z^{exp.}} \times 100$$

where $X\widehat{-Y-}Z^{exp.}$ (respectively $X\widehat{-Y-}Z^{calc.}$) represents the experimental (respectively calculated) angle.

a. Influence of the functional in combination with the 6-311++G(2d,2p) basis set

To begin with, the effects of the density functionals on representative geometric parameters were studied in the case of the Ti^{+III}(1) compound. The experimental data were taken from Ref.[23] The main results are shown in the Table 1.

The experimental Ti-N and Ti-B distances are $d_{Ti-N}^{exp.} = 2.153$ and $d_{Ti-B}^{exp.} = 2.520$ Å, respectively. The corresponding values are calculated to be in the [2.155 Å; 2.184 Å], and [2.501 Å ; 2.542 Å] ranges, respectively. The δd_{Ti-N} deviation between the experimental and the calculated distance is thus in the [+0.1% ; +1.5%] range, whereas the δd_{Ti-B} deviation is in the [-0.8% ; 0.9%] range. Thus, the calculated $d_{Ti-N}^{calc.}$ and $d_{Ti-B}^{calc.}$ distances are in good agreement with the experimental data.

With all the levels of theories used, the two B-H bonds that are not interacting with the Ti atom are calculated to be identical in length. However, from crystallographic structures, two different lengths are measured for these non-agostic B-H bonds: 1.09 and 1.13 Å. This suggests the existence of additional weak intermolecular interactions either with the solvent during the evaporation, or between molecules in the solid phase.

The corresponding calculated distance ($d_{B-H}^{calc.}$) is in the [1.200 Å ; 1.212 Å] range. Thus, the deviation between the experimental and the calculated B-H distance, is in the [8.2% ; 9.2%] range. The deviation observed between the experimental and the calculated B-H distance is much larger than the deviation obtained for the Ti-N and Ti-B distances. Such discrepancy may be due to the uncertainty in the crystallographic data, especially concerning the location of the hydrogen atoms.

	d_{Ti-N}	d_{Ti-B}	d_{B-H}	$d_{B-H\ agost.}$	Δd_{B-H} [(a)]	$d_{Ti-H\ agost.}$	$B-\widehat{H_{agost.}-T}$	$Ti-\widehat{N-B}$	$N-\widehat{B-H_{agost.}}$	Dev_{tot} (%)[(b)]
BP86-D3	**2.173**/*2.203*	**2.514**/*2.552*	**1.211**/*1.212*	**1.311**/*1.309*	**0.100**/0.097	**1.872**/*1.878*	**102.9**/*105.0*	**83.1**/*84.4*	**105.6**/*104.5*	**4.3**
BP86	**2.184**/*2.203*	**2.530**/*2.552*	**1.212**/*1.212*	**1.312**/*1.309*	**0.100**/0.097	**1.882**/*1.878*	**103.4**/*105.3*	**83.4**/*84.6*	**105.4**/*104.3*	**4.6**
TPSSTPSS-D3	**2.172**/*2.198*	**2.519**/*2.544*	**1.205**/*1.205*	**1.304**/*1.304*	**0.099**/0.099	**1.870**/*1.873*	**103.6**/*105.6*	**83.2**/*84.5*	**105.0**/*103.8*	**5.4**
TPSSTPSS	**2.181**/*2.207*	**2.532**/*2.567*	**1.205**/*1.206*	**1.305**/*1.306*	**0.100**/0.100	**1.878**/*1.882*	**103.9**/*105.9*	**83.4**/*84.7*	**104.9**/*103.7*	**5.1**
B3PW91	**2.170**/*2.193*	**2.519**/*2.552*	**1.206**/*1.206*	**1.303**/*1.303*	**0.097**/*0.097*	**1.880**/*1.881*	**103.1**/*105.1*	**83.6**/*84.8*	**105.5**/*104.3*	**6.4**
PBE1PBE	**2.163**/*2.184*	**2.510**/*2.542*	**1.207**/*1.208*	**1.303**/*1.303*	**0.096**/0.095	**1.879**/*1.878*	**102.7**/*104.6*	**83.5**/*84.7*	**105.7**/*104.5*	**7.4**
TPSSh	**2.174**/*2.197*	**2.526**/*2.559*	**1.204**/*1.205*	**1.302**/*1.304*	**0.098**/0.099	**1.877**/*1.878*	**103.7**/*105.6*	**83.5**/*84.8*	**104.9**/*103.7*	**6.5**
PBE1PBE-D3	**2.157**/*2.179*	**2.502**/*2.534*	**1.207**/*1.207*	**1.302**/*1.302*	**0.095**/0.095	**1.874**/*1.873*	**102.5**/*104.3*	**83.3**/*84.4*	**105.8**/*104.6*	**8.5**
LC-ωPBE-D3	**2.150**/*2.166*	**2.492**/*2.522*	**1.206**/*1.206*	**1.297**/*1.294*	**0.091**/0.088	**1.871**/*1.869*	**102.2**/*104.3*	**83.1**/*84.4*	**106.0**/*104.6*	**12.9**
LC-ωPBE	**2.155**/*2.171*	**2.501**/*2.531*	**1.206**/*1.206*	**1.297**/*1.295*	**0.091**/0.089	**1.877**/*1.875*	**102.4**/*104.4*	**83.2**/*84.6*	**105.9**/*104.5*	**12.5**
M06	**2.163**/*2.182*	**2.517**/*2.554*	**1.204**/*1.205*	**1.294**/*1.290*	**0.090**/*0.085*	**1.892**/*1.901*	**102.8**/*104.7*	**83.6**/*85.1*	**105.7**/*104.4*	**13.0**
B3LYP-D3	**2.171**/*2.195*	**2.524**/*2.558*	**1.202**/*1.202*	**1.295**/*1.294*	**0.093**/0.092	**1.883**/*1.885*	**103.6**/*105.7*	**83.6**/*84.9*	**105.1**/*103.9*	**10.9**
B3LYP	**2.182**/*2.207*	**2.542**/*2.576*	**1.203**/*1.203*	**1.297**/*1.297*	**0.094**/0.094	**1.895**/*1.898*	**104.0**/*105.9*	**84.0**/*85.2*	**104.9**/*103.7*	**10.9**
M06-L	**2.178**/*2.197*	**2.525**/*2.561*	**1.200**/*1.201*	**1.282**/*1.280*	**0.082**/0.079	**1.899**/*1.909*	**103.4**/*105.1*	**83.4**/*84.9*	**105.8**/*104.7*	**21.9**
Exp	**2.153**	**2.52**	**1.13 & 1.09**	**1.21**	**0.1**			**84.5**	**107.1**	

Table 1: Influence of the functional on the geometric description of the Ti^{+III}(1) (in bold) and Ti_e^{+IV}(1) (in italic) compounds. The distances are in Å, and the angles are in Degrees. [(a)]: $\Delta d_{B-H} = (d_{B-Hagost.} - d_{B-H.})$, [(b)]: $Dev_{tot} = |\delta d_{Ti-N}| + |\delta d_{Ti-B}| + |\delta \Delta d_{B-H}| + |\delta_{Ti-N-B}| + \left|\delta_{N-B-H_{agost.}}\right|$, with $\delta_{\Delta d_{B-H}} = \frac{\Delta d_{B-H}^{calc.} - \Delta d_{B-H}^{exp.}}{\Delta d_{B-H}^{exp.}} \times 100$ All the calculations were carried out with the triple-ζ 6-311++ G(2d,2p) basis set. The different functionals are classified from smaller to larger Dev_{tot}values. All the calculations were carried out with the 6-311++G(2d,2p) basis set.

In the case of the B-H bond involved in the agostic interaction, the experimental distance is 1.21 Å while the corresponding $d^{calc.}_{B-H\ agost.}$ calculated distance is in the [1.282 Å; 1.312 Å] range. Thus, the δ $d_{B\text{-}H\ agost.}$ deviation between the experimental and the calculated B-H distance, is in the [6.0%; 8.5%] range. It is interesting to note that the deviation between the calculated and the experimental distance is similar to the one obtained in the case of the non-agostic B-H bond. To further characterize the 3C/2e interaction, we calculated the difference between the length of the agostic B-H bond and the free B-H bond. This lengthening is of 0.10 Å for the experimental data, and in the range 0.079 -0.100 Å, for the calculated distances. Thus, the δ $\Delta d_{B\text{-}H}$ deviation between the experimental and the calculated difference is in the [-18.0% ; 0%] range, with:

$$\delta\Delta d_{B-H} = \frac{\left(d^{calc.}_{B-H\ agost.} - d^{calc.}_{B-H.}\right) - \left(d^{exp.}_{B-H\ agost.} - d^{exp.}_{B-H}\right)}{\left(d^{exp.}_{B-H\ agost.} - d^{exp.}_{B-H}\right)} \times 100$$

We thus conclude that the lengthening of the B-H bond due to the interaction with the metallic centre is correctly described by all the selected functionals, with a deviation of $\pm$ 0.03 Å depending on the functional used.

In addition with distances, the angles are often used as criteria in the identification of agostic bondings. In the case of σ(C-H) bonds, it is generally considered that a $Ti\widehat{-H-C}$ angle in the [90°; 140°] range corresponds to an agostic interaction. Furthermore, a $Ti\widehat{-H-C}$ angle in the [110°; 170°] range is generally attributed to an anagostic interaction.[9]

The $M\widehat{-H-B}$ angles reported in the Table 1 show that, in the case of the titanocene amino-borane, the $M\widehat{-H-B}$ angle is calculated in the [102.2°; 104.0°] range, whatever the functional used. Thus, the geometries calculated with all the chosen functional are consistent with the formation of an agostic interaction between the σ(B-H) bond and the titanium atom.

The calculated values for the $Ti\widehat{-N-B}$ angle are in the [81.3°; 84.0°] range, whereas the experimental value is 84.5°. This angle is thus systematically calculated smaller than the experimental value, and the deviation between the experimental and the calculated value is in the [-3.79% **;** -0.59%] range.

Similarly, the calculated $N-B\widehat{-H}_{agostic}$ angle is calculated in the [104.5°; 105.9°] range, which is systematically larger than the corresponding experimental value ($N-B\widehat{-H}_{agostic}{}^{exp.} = 107.1°$), and the $\delta_{N-B-H_{agost.}}$ deviation between the experimental and the theoretical value is in the [-2.1%; -1.2%] range. For a whole comparison of the functionals, a new parameter was introduced the total deviation Dev_{tot} :

$$Dev_{tot} = |\,\delta d_{Ti-N}| + |\,\delta d_{Ti-B}| + |\,\delta\Delta d_{B-H}| + |\,\delta_{Ti-N-B}| + \left|\,\delta_{N-B-H_{agost.}}\right|$$

Dev_{tot} is a measure of the normalized total deviation between the calculated and the experimental values, based on two distances (d_{Ti-N} and d_{Ti-B}), one reduced distance (Δd_{B-H}) and two angles ($Ti\widehat{-N-B}$ and $N-B\widehat{-H}_{agost.}$). In the Table 1, the different functionals are classified from the one leading to the smaller Dev_{tot} to the one leading to the larger Dev_{tot}. The smallest Dev_{tot} value is obtained with the BP86 functional (with or without the use of the D3 empirical correction of Grimme with Becke and Johnson damping), whereas the use of the M06-L functional leads to the larger Dev_{tot} value. Moreover, the Dev_{tot} values are below 25 % for all the considered functionals. Thus, from a geometric point of view, the 12 chosen functionals correctly describe the Ti^{+III}(1) compound. Two major points will be further discussed: the influence of the use of the D3 empirical correction of Grimme with Becke and Johnson damping, and the effect of the class (local, GGA, hybrid GGA, meta-GGA and range-separated hybrids) of the functionals on the geometric description of this system.

1. *Influence of the D3 empirical correction of Grimme with Becke and Johnson damping*

The agostic interaction has often been compared to the hydrogen bond. In the latter case, the dispersion forces may notably contribute to the stabilization of the system. A substantial effort was recently made to take into account these forces in DFT calculations. In the present study, the effect of the D3 empirical correction of Grimme with Becke

and Johnson damping was evaluated in the case of one GGA functional (BP86), two hybrid functionals (PBE1PBE and B3LYP), and one meta-GGA (TPSSTPSS) and one range-separated hybrid functional (LC-ωPBE). To evaluate the effect of the D3 empirical correction of Grimme with Becke and Johnson damping, the difference between the selected distances and angles calculated with and without this correction are presented in the Table **S1**.

Four tendencies can be drawn from these comparisons:

- For a given functional, the use of the D3 empirical correction of Grimme with Becke and Johnson damping systematically leads to smaller Ti-N and Ti-B distances. However, this shortening remains smaller than 0.02 Å with the five considered functionals,
- The D3 empirical correction of Grimme with Becke and Johnson damping has almost no effect on the B-H and B-$H_{agost.}$ distances,
- The Ti-$H_{agost.}$ distance is systematically predicted to be smaller when the D3 empirical correction of Grimme with Becke and Johnson damping is used. As in the case of the Ti-N and Ti-B distances, this shortening remains smaller than 0.02 Å with the five considered functionals,
- The angles $\mathrm{B-\widehat{H_{agost.}-Ti}}$ and $\mathrm{Ti-\widehat{N-B}}$ are predicted to be 0.1 to 0.5° larger when geometry optimizations are carried out without the D3 correction. Conversely, the $\mathrm{N-\widehat{B-H_{agost.}}}$ is predicted to be 0.1 to 0.2° larger when the D3 correction is used.

Thus, the use of the D3 empirical correction of Grimme with Becke and Johnson damping do not dramatically affect the geometry of the Ti^{+III}(1) compound, and "classical" DFT calculations can suitably describe this 3C/2e interaction. This suggests that the dispersive forces do not play a prominent role in the agostic interaction herein investigated.

2. *<u>Comparison of the calculated geometric parameters depending on the class of the functional used</u>*

In our prototype system, the electrostatic nature of the interaction may play a predominant role. Thus, in the context of DFT studies, the treatment of the electron correlation may affect the description of the interaction. More precisely, we were interested in the influence of the class of the functional on the accuracy of the geometric description of the interaction. The deviation of distances and angles with the experimental data are shown in the Table **S2** for each class of functionals:

- in the case of the local M06-L functional, the deviation on the Ti-N distance is five times higher than that on the Ti-B distance. This functional leads to the highest value of $\mathrm{Dev_{tot}}$ parameter among the considered functionals,
- the GGA BP86 functional leads to an accurate geometric description of the system, and the $\mathrm{Dev_{tot}}$ parameter is particularly low, suggesting that this functional is particularly adapted for the description of the system,
- the GGA BP86-D3 functional also leads to an accurate description of the interaction. On the other hand, the Ti-N distance is slightly overestimated, whereas the Ti-B distance is slightly underestimated,
- the hybrid B3LYP functional leads to a similar overestimation of the Ti-N and Ti-B distances. In the same time, the lengthening of the B-H bond due to the agostic interaction is correctly reproduced,
- the combination of this functional with the D3 empirical correction of Grimme with Becke and Johnson damping does not lead to a decrease of the $\mathrm{Dev_{tot}}$ parameter,
- the hybrid PBE1PBE functional, taken alone or with the D3 empirical correction of Grimme with Becke and Johnson damping, leads to an overestimation of the Ti-N distance, whereas the Ti-B distance is underestimated,
- in the case of the TPSSh hybrid functional, the deviation on the Ti-N distance is almost three times larger than the deviation on the Ti-B distance,
- the meta-GGA TPSSTPPS and TPSSTPSS-D3 functionals also lead to an overestimation of the Ti-N distance that is much higher than the deviation on the Ti-B distance,

- the range-separated LC-ωPBE and LC-ωPBE-D3 hybrid functionals lead to an underestimation of the Ti-B distance that is much more important than the deviation on the Ti-N distance.

Finally, only two functionals lead to a similar deviation of the Ti-N and Ti-B distances, in combination with an accurate lengthening of the B-H bond involved in the agostic interaction, and with a low value of the $\mathrm{Dev_{tot}}$ parameter: the GGA BP86 functional, and the hybrid B3LYP functional. If we consider a $\pm$ 0.03 Å uncertainty for distances and a $\pm$ 3° uncertainty for angles as acceptable, then the popular B3LYP hybrid functional satisfactorily describe the Ti^{+III}(1) compound. This functional was selected for the further evaluation of the effects of basis sets.

In the Table 1 are also reported the calculated geometric parameters for the $\mathrm{Ti_e^{+IV}}$(1) compound. As in the case of the Ti^{+III}(1) compound, no dramatic change is observed with respect to the choice of the functional. No experimental data are available for this system, but these results show that all the considered functionals lead to a similar geometric description of the Ti^{+III}(1) and $\mathrm{Ti_e^{+IV}}$(1) compounds. More precisely, the variations of the calculated distances and angles for the Ti^{+III}(1) and $\mathrm{Ti_e^{+IV}}$(1) compounds are presented in the Table **S3** The calculated Ti-N and Ti-B distances are systematically longer in the diamagnetic $\mathrm{Ti_e^{+IV}}$(1) compound with respect to the paramagnetic Ti^{+III}(1) species: $\Delta_{\mathrm{Ti-N}}^{\mathrm{IV-III}}$ and $\Delta_{\mathrm{Ti-B}}^{\mathrm{IV-III}}$ are in the [0.016 Å ; 0.030 Å] and [0.022 Å ; 0.038 Å] ranges, respectively, with:

$$\Delta_{\mathrm{Ti-N}}^{\mathrm{IV-III}} = \mathrm{d}_{\mathrm{Ti-N}}^{\mathrm{diamagnetic}} - \mathrm{d}_{\mathrm{Ti-N}}^{\mathrm{paramagnetic}} \quad \text{and} \quad \Delta_{\mathrm{Ti-B}}^{\mathrm{IV-III}} = \mathrm{d}_{\mathrm{Ti-B}}^{\mathrm{diamagnetic}} - \mathrm{d}_{\mathrm{Ti-B}}^{\mathrm{paramagnetic}}$$

The M06-L, BP86, LC-ωPBE and LC-ωPBE-D3 functionals lead to the lower $\Delta_{\mathrm{Ti-N}}^{\mathrm{IV-III}}$ values.

Thus, the theoretical calculations suggest that, in the case of the E isomer, the magnetic properties of the titanium atom do not affect the agostic and non-agostic B-H distances in the titanocene (1) complexes.

b. Influence of the basis set and of the relativistic treatment in combination with the B3LYP functional

The Ti^{+III}(1) and $\mathrm{Ti_e^{+IV}}$(1) compounds were chosen as case studies, because in addition with experimental data available for the Ti^{+III}(1) compound, a large choice of basis sets is available, including triple- and quadruple-ζ all electron basis sets and relativistic pseudopotentials. However, for organometallic complexes containing heavier group 4 metallic centres, pseudopotentials should be used for calculations in currently available calculators, in order to reduce the number of primitive Gaussians. Moreover, relativistic effects are obviously non-negligible in the case of organometallic complexes. In addition with relativistic pseudopotentials (SDD and LanL2DZ), the scalar relativistic Douglas-Kroll-Hess Hamiltonian was used.

As in the case of the study of the effect of the functional on the geometric description of the agostic interaction, the choice of the basis set does not affect the angles between the B, N, H and Ti atoms. The effects of the basis set on the previously chosen distances are presented in the Table 2. At a first glance, it appears that the Ti-N and Ti-B experimental distances are correctly reproduced, with a deviation of ± 0.03 Å. The lengthening of the B-H bond involved in the agostic interaction is also correctly reproduced, with a deviation of ± 0.01 Å. Thus, from a geometrical point of view, all the considered basis sets combined with the B3LYP functional lead to a suitable description of the Ti^{+III}(1) system.

Four Alrichs' basis sets were chosen for this study: Def2-TZVP, Def2-TZVPP, Def2-TZVPPD and Def2-QZVP. Very similar geometries were obtained will these four basis sets: the Ti-N distance is calculated to be 2.182 with all these basis sets, whereas the Ti-B distance is calculated to be in the [2.539 Å; 2.541 Å]. This corresponds to a slight overestimation of the experimental distances, and the deviations between the theoretical and experimental values is +1.4% for the Ti-N distance, and in the [0.8% ; 0.9%] range for the Ti-B distance.

These Alrichs' basis sets also lead to an underestimation of the lengthening of the B-H bond due to the agostic interaction, and the $\delta_{\Delta dB\text{-}H}$ is in the [-7.0% ; -5.0%] range, with:

$$\delta_{\Delta \mathbf{d}_{\mathbf{B-H}}} = \frac{\Delta \mathbf{d}_{\mathbf{B-H}}{}^{\text{calc.}} - \Delta \mathbf{d}_{\mathbf{B-H}}{}^{\text{exp.}}}{\Delta \mathbf{d}_{\mathbf{B-H}}{}^{\text{exp.}}} \times 100$$

Two Pople's basis sets were considered in our study: the 6-311++G(2d,2p) basis set, alone and in combination with the D3 empirical correction of Grimme with Becke and Johnson damping, and the 6-311++G(3df,3pd) basis set. As in the case of the Alrichs' basis sets, the Ti-N and Ti-B distances are slightly overestimated, and the $\delta d_{\text{Ti-N}}$ and $\delta d_{\text{Ti-B}}$ are in the [+0.9% ; +1.4%] and [+0.8% ; +1.0%] ranges, respectively. The lengthening of the B-H bond due to the agostic interaction is underestimated with these basis sets, and the $\delta_{\Delta \mathbf{d}_{\mathbf{B-H}}}$ is in the [-9.0% ; -7.0%] range.

The use of either LanL2DZ or SDD pseudopotential for the metallic centre, in combination with the 6-311++G(2d,2p) basis set for the other atoms, leads to an improvement of the accuracy of the calculated distances. The use of the LanL2DZ pseudopotential for the metallic centre in combination with the D3 empirical correction of Grimme with Becke and Johnson damping, leads to an overestimation of the Ti-N distance, and an underestimation of the Ti-B distance.

The influence of the use of a scalar relativistic Hamiltonian was also studied. To this end, the two-component relativistic Douglas-Kroll-Hess Hamiltonian was considered, in combination with the DZP-DKH and TZP-DKH basis sets. For a sake of comparison, non-relativistic calculations were also carried out with the DZP and TZP basis sets. Due to a limitation of variables for such calculations with the Guassian09 software, only partial optimizations were carried out. All but nine parameters were frozen, and the positions of the Ti, N, B and H atoms were optimized. The same variables were frozen for the relativistic DKH2/DZP-DKH, DKH2/TZP-DKH and for the non-relativistic DZP and TZP calculations. In the case of the non-relativistic DZP calculations, the Ti-N and Ti-B distances are 2.176 and 2.540 Å, respectively. Compared with the experimental data, this corresponds to a slight overestimation. ($\delta d_{\text{Ti-N}}$ = 1.1 % and $\delta d_{\text{Ti-B}}$ = 0.8 %). The lengthening of the B-H bond involved in the agostic interaction is also slightly overestimated ($\delta_{\Delta dB\text{-}H}$ = 8.0 %). Similar distances are calculated when this basis set is used in the context of relativistic DKH calculations ($\delta d_{\text{Ti-N}}$ = 1.0 %, $\delta d_{\text{Ti-B}}$ = 0.63 % and $\delta_{\Delta \mathbf{d}_{\mathbf{B-H}}}$ = 10.0 %). No dramatic change is observed between the structures partially optimized at the B3LYP/DZP (respectively B3LYP/TZP) level of theory and the structures partially optimized at the relativistic DKH2 B3LYP/DZP-DKH (respectively B3LYP/TZP-DKH) level of theory. This suggests that the relativistic effect has a limited impact on the agostic interaction in the Ti^{+III}(1) compound.

Thus, among the functionals and the basis sets selected for our study, all the levels of theory tested lead to an accurate description of the agostic interaction in the Ti^{+III}(1) compound, from a geometric point of view. The Ti-N, Ti-B and the lengthening of the B-H bond due to the agostic interaction are reproduced with an accuracy better than ± 0.04 Å with all the considered DFT methods. The effect of the method on the topological characterization of the interactions will be further investigated.

Type of basis set	Basis set	d_{Ti-N}	d_{Ti-B}	d_{B-H}	$d_{B-H\ agost.}$	Δd_{B-H} [a]	$d_{Ti-H\ agost.}$
Alrichs' basis sets	Def2-TZVP	**2.182/***2.207*	**2.540/***2.574*	**1.204/***1.205*	**1.299/***1.299*	**0.095**	**1.894/***1.895*
	Def2-TZVPP	**2.182/***2.207*	**2.541/***2.575*	**1.203/***1.204*	**1.298/***1.297*	**0.095**	**1.895/***1.898*
	Def2-QZVPP	**2.182/***2.201*	**2.540/***2.575*	**1.202/***1.203*	**1.297/***1.297*	**0.095**	**1.894/***1.897*
Pople's basis sets	6-311++G(2d,2p)	**2.182/***2.207*	**2.542/***2.576*	**1.202/***1.203*	**1.297/***1.297*	**0.095**	**1.895/***1.898*
	6-311++G(3df,3pd)	**2.182/***2.206*	**2.540/***2.574*	**1.203/***1.203*	**1.297/***1.297*	**0.094**	**1.894/***1.897*
Pople basis sets with a relativistic pseudopotential for the metallic centre	6-311++G(2d,2p)+LanL2DZ	**2.177/***2.204*	**2.529/***2.556*	**1.202/***1.203*	**1.298/***1.299*	**0.096**	**1.879/***1.885*
	6-311++G(2d,2p)+SDD	**2.174/***2.199*	**2.535/***2.571*	**1.202/***1.203*	**1.297/***1.297*	**0.095**	**1.889/***1.893*
Double and triple zeta basis sets	DZP(9v)	**2.176/***2.203*	**2.540/***2.581*	**1.219/***1.219*	**1.312/***1.310*	**0.093**	**1.894/***1.899*
	DKH2/DZP-DKH (9v)	**2.173/***2.201*	**2.536/***2.582*	**1.219/***1.219*	**1.314/***1.311*	**0.095**	**1.890/***1.899*
	RESC/DZP-DKH(9v)	**2.174/***2.201*	**2.537/***2.582*	**1.219/***1.219*	**1.314/***1.311*	**0.095**	**1.891/***1.899*
	TZP(9v)	**2.183/***2.211*	**2.539/***2.275*	**1.204/***1.204*	**1.301/***1.300*	**0.097**	**1.887/***1.891*
	DKH2/TZP-DKH (9v)	**2.180/***2.209*	**2.535/***2.576*	**1.204/***1.204*	**1.300/***1.299*	**0.096**	**1.885/***1.892*
Exp		**2.153**	**2.52**	**1.13 & 1.09**	**1.21**	**0.1**	

Table 2: Effect of the basis set on the geometric description of the Ti^{+III}(1) and Ti_e^{+IV}(1) compounds. The distances are in Å, and the angles are in Degrees.

[(a)]: $\Delta d_{B-H} = (d_{B-Hagost.} - d_{B-H.})$. All the calculations were carried out with the B3LYP functional.

2. Topological characterization of the 3C/2e interaction

For the characterization of a 3C/2e and an estimation of the strength of an agostic interaction, the previously proposed methodology consists in studying the protonated basin.[66] We shall briefly remind the reader of the main steps of this topological methodology.

First of all, the 3C/2e nature of the interactions should be ascertained. To this end, the protonated basin within the ELF topological framework should be a trisynaptic basin with a total population close to 2 electrons. Then, a QTAIM/ELF study is carried out to determine the atomic contributions of the metallic centre, the hydrogen atom and the boron atom in the present case, to the protonated basin. The strength of the agostic interaction is evaluated on the basis of the atomic contribution of the metallic centre. Thus, besides an accurate geometric characterization of the organometallic complex, the electronic description of the system obtained from DFT calculations should be precise enough prior to the topological investigation. To evaluate the accuracy of this description, the topological characterization of the protonated basin involved in the agostic interaction was studied for the Ti^{+III}(1) and Ti_e^{+IV}(1) compounds:

- with all the above considered functionals in combination with the 6-311++G(2d,2p) basis set,
- with all the above considered basis sets, in combination with the B3LYP functional.

a. Influence of the functional in combination with the 6-311++G(2d,2p) basis set

The influence of the choice of the functional on the topological description of the protonated basins, for the hydrogen atoms involved in the agostic interaction, was studied in the context of DFT calculations with the 6-311++G(2d,2p) basis set. The characteristic results obtained for the Ti^{+III}(1) and Ti_e^{+IV}(1) compounds are summarized in the Table 3.

First of all, we would like to underline the fact that, whatever the functional used with the 6-311++G(2d,2p) basis set, the hydrogen atom involved in the agostic interaction is characterized, within the ELF topological framework, by a trisynaptic protonated basin with a total population in the $1.92 \leq V(Ha) \leq 1.94$ electron range, for the Ti^{+III}(1) compound. This is fully consistent with a 3C/2e interaction. Thus, the analysis of the topology of the electron density and the electron density ELF function indeed demonstrates the presence of an agostic interaction between a σ(B-H) bond and the titanium atom. The contribution of the titanium atom in this basin, noted V(Ha)-M, varies from 0.11 to 0.14 electron. The lowest value is calculated with the M-06L/6-311++G(2d,2p) level of theory, whereas the highest value is obtained with the BP86/6-311++G(2d,2p) and BP86-D3/6-311++G(2d,2p) levels of theory. With all the other functionals, the calculated contribution of the metallic centre in the protonated basin (V(Ha)-M) is calculated in the [0.12 e; 0.13 e] range for the Ti^{+III}(1) compound, depending on the functional.

With all the levels of theory presented in the Table 3, the total population of the hydrogen atom is smaller in the case of the Ti_e^{+IV}(1) compound, and V(Ha) is calculated in the [1.88 e ; 1.90 e] range. However, as in the previous case, a trisynaptic basin is obtained, in full agreement with a 3C/2e agostic interaction. The atomic contribution of the metallic centre within this protonated basin is calculated to be in the [0.10 e; 0.12 e] range for the Ti_e^{+IV}(1) compound, with all the considered functionals.

Thus, consistent descriptions of the agostic interactions are obtained from the topological QTAIM/ELF approach. The M06-L/6-311++G(2d,2p) level of theory is likely to slightly underestimate the strength of the agostic interaction in the Ti^{+III}(1) compound. On the contrary, the BP86/6-311++G(2d,2p) and BP86-D3/6-311++G(2d,2p) levels of theory probably slightly overestimate the strength of the agostic interaction in the Ti^{+III}(1) compound. Globally, the strengths of the agostic interactions in the Ti^{+III}(1) and Ti_e^{+IV}(1) compounds are calculated to be very

similar, in full agreement with the geometric data. It seems however that the agostic interaction may be slightly higher in the case of the Ti^{+III}(1) compound. Indeed, if we exclude the LC-ω-PBE-D3/6-311++G(2d,2p) level of theory, the contribution of the metallic centre on the protonated basin is systematically slightly higher, by 0.01 to 0.03 electron, in the case of the Ti^{+III}(1) compound.

	V(Ha)	Atomic contribution		
		V(Ha)-Ti	V(Ha)-B	V(Ha)-Ha
B3LYP	**1.93**/*1.89*	**0.12**/*0.10*	**0.24**/*0.23*	**1.56**/*1.53*
B3LYP-D3	**1.93**/*1.90*	**0.12**/*0.11*	**0.24**/*0.24*	**1.55**/*1.54*
B3PW91	**1.93**/*1.89*	**0.13**/*0.11*	**0.25**/*0.26*	**1.54**/*1.52*
TPSSh	**1.93**/*1.89*	**0.12**/*0.11*	**0.22**/*0.22*	**1.55**/*1.55*
TPSSTPSS	**1.93**/*1.89*	**0.12**/*0.10*	**0.23**/*0.23*	**1.55**/*1.54*
TPSSTPSS-D3	**1.93**/*1.89*	**0.13**/*0.11*	**0.23**/*0.22*	**1.55**/*1.54*
M06-L	**1.94**/*1.90*	**0.11**/*0.10*	**0.24**/*0.22*	**1.57**/*1.56*
M06	**1.93**/*1.89*	**0.12**/*0.11*	**0.25**/*0.24*	**1.55**/*1.54*
BP86	**1.92**/*1.88*	**0.14**/*0.12*	**0.26**/*0.25*	**1.51**/*1.50*
BP86-D3	**1.92**/*1.88*	**0.14**/*0.11*	**0.25**/*0.25*	**1.51**/*1.49*
LC-ωPBE	**1.94**/*1.90*	**0.12**/*0.11*	**0.24**/*0.23*	**1.56**/*1.53*
LC-ωPBE-D3	**1.94**/*1.89*	**0.12**/*0.12*	**0.23**/*0.22*	**1.56**/*1.53*
PBE1PBE	**1.93**/*1.89*	**0.13**/*0.11*	**0.24**/*0.23*	**1.55**/*1.52*
PBE1PBE-D3	**1.94**/*1.89*	**0.13**/*0.11*	**0.24**/*0.23*	**1.55**/*1.52*

Table 3: Effect of the functional on the ELF topological description of the protonated basin for the hydrogen atom involved in the agostic interaction with the metallic centre, in the Ti^{+III}(1), in bold, and Ti_e^{+IV}(1), in italic, compounds. All the calculations were carried out with the 6-311++G(2d,2p) basis set.

The B3LYP functional, previously selected on the basis of geometric criteria, seems to satisfactorily describe the agostic interaction of the Ti^{+III}(1) and Ti_e^{+IV}(1) compounds , from an electronic, topological point of view.

b. Influence of the basis set in combination with the B3LYP functional

As in the case of the geometric study, the B3LYP functional was further selected to evaluate the influence of the basis set on the electronic characterization of the agostic interaction. The main results are presented in the Table 4.

With all the basis sets selected for this study, calculations carried out with the B3LYP functional leads to the characterization of a trisynaptic protonated basin with a total population in the [1.92 e; 1.94 e] range, for the paramagnetic Ti^{+III}(1) compound. Thus, whatever the level of theory chosen, the topological analysis leads to the identification of a 3C/2e agostic interaction. However, the calculated contribution of the metallic centre on this protonated basin very much depends on the basis set. At the B3LYP/6-311++G(2d,2p)+LanL2DZ, B3LYP-D3/6-311++G(2d,2p)+LanL2DZ and B3LYP/6-311++G(2d,2p)+SDD levels of theory, the atomic contribution of the Ti atom in the hydrogen atom, is calculated to be in the [0.06 e; 0.07 e]. With all the other selected basis sets, i.e. without the use of a pseudopotential for the metallic atom, the atomic contribution of the Ti atom in the hydrogen atom, is calculated to be 0.12 electron. We thus conclude that the use of a relativistic pseudopotential for the metallic centre leads to an accurate description of the agostic interaction from a geometric point of view, but not from a topological point of view. The use of a basis set that takes into account the core electrons is

necessary prior to any topological investigation of an agostic interaction. For a sake of computational time saving, we carried out a single point calculation with the relativistic DKH2/DZP-DKH basis set, at the geometry optimized with the B3LYP functional, in combination with the LanL2DZ basis set for the metallic atom and the 6-311++G(2d,2p) basis set for all the other atoms. When the topological study is carried out from this single point calculation, the atomic contribution of the metallic centre in the trisynaptic agostic basin is calculated to be 0.11 electron. Thus, a single point calculation using the DKH2 Hamiltonian in combination with the B3LYP/DZP-DKH level of theory from a correct geometry obtained with a pseudopotential for the metallic centre is sufficient to accurately describe the agostic interaction from a topological point of view. Since the DKH2/DZP-DKH basis set is available for all the atoms involved in the compounds selected for the present study, the following procedure will be further considered:

1. a geometry optimization with the B3LYP functional, in combination with the LanL2DZ basis set for the metallic atom and the 6-311++G(2d,2p) basis set for all the other atoms,
2. a single point calculation using the DKH2 Hamiltonian in combination with the B3LYP/DZP-DKH level of theory,
3. the generation of a *.wfn* file that will be further used for the topological study of the agostic interaction,
4. the ELF identification of a trisynaptic protonated basin.

We would like to point out the fact that the use of the DKH2 and RESC Hamiltonians lead to similar description of the agostic interaction in terms of geometric as well as topological descriptors, and the use of the RESC Hamiltonian is much less time consuming than the DKH2 one.

	V(Ha)	Atomic contribution		
		V(Ha)-Ti	V(Ha)-B	V(Ha)-Ha
6-311++G(2d,2p)+LanL2DZ	**1.92**/*1.89*	**0.06**/*0.06*	**0.23**/*0.23*	**1.61**/*1.58*
6-311++G(2d,2p)+SDD	**1.93**/*1.89*	**0.06**/*0.07*	**0.24**/*0.23*	**1.61**/*1.58*
6-311++G(2d,2p)	**1.93**/*1.89*	**0.12**/*0.10*	**0.24**/*0.23*	**1.56***1.53*
6-311++G(3df,3pd)	**1.93**/*1.88*	**0.12**/*0.10*	**0.23**/*0.23*	**1.56**/*1.54*
Def2-TZVP	**1.92**/*1.88*	**0.12**/*0.10*	**0.23**/*0.22*	**1.56**/*1.54*
Def2-TZVPP	**1.92**/*1.89*	**0.12**/*0.10*	**0.23**/*0.22*	**1.56**/*1.54*
Def2-TZVPPD	**/***1.89*	**/***0.11*	**/***0.22*	**/***1.54*
Def2-QZVPP	**1.92**/*1.89*	**0.12**/*0.10*	**0.23**/*0.23*	**1.57**/*1.57*
DKH2/DZP-DKH (9v)	**1.94**/*1.89*	**0.12**/*0.10*	**0.21**/*0.19*	**1.58**/*1.57*
RESC/DZP-DKH(9v)	**1.94**/*1.89*	**0.12**/*0.10*	**0.24**/*0.22*	**1.58**/*1.57*
DKH2/TZP-DKH (9v)	**1.94**/*1.89*	**0.12**/*0.10*	**0.23**/*0.21*	**1.56**/*1.55*
DZP(9v)	**1.94**/*1.89*	**0.12**/*0.10*	**0.22**/*0.20*	**1.58**/*156*
TZP(9v)	**1.94**/*1.89*	**0.12**/*0.10*	**0.23**/*0.21*	**1.58**/*1.55*
6-311++G(2d,2p)+LanL2DZ + single point with DKH2/DZP-DKH	**1.93**/*1.89*	**0.11**/*0.10*	**0.21**/*0.21*	**1.59**/*1.57*

Table 4: Effect of the basis set on the ELF topological description of the protonated basin for the hydrogen atom involved in the agostic interaction with the metallic centre, in the Ti^{+III}(1), in bold, and Ti_e^{+IV}(1), in italic, compounds. All the calculations were carried out with the B3LYP functional. All the values are given in e.

Furthermore, for the present study, we can anticipate that the QTAIM topological approach is a straightforward tool for a comparison of the agostic strength, since only β-agostic interactions are considered in the present study. Such interactions are generally characterized by a bond critical point (BCP) between the hydrogen involved in the interaction and the metallic centre. For the sake of clarity, this BCP will be further denoted as $BCP_{M\text{-}H\ agostic}$. The electron density ρ, the Laplacian of the electron density $\nabla^2\rho$, the ellipticity ε, and the total energy density H, at this $BCP_{M\text{-}H\ agostic}$ can be used for an accurate description of the interaction.

3. Characterization of the strength of the interaction

a. Influence of the functional in combination with the 6-311++G(2d,2p) basis set

Before using the QTAIM approach to estimate the strength of agostic interactions, one initial point to consider is the impact of the level of theory on the accuracy of the QTAIM topological description of (i) the free B-H bonds, (ii) the agostic B-H bond and (iii) the M-H interaction. The results obtained for the Ti^{+III}(1) compound with the selected functionals in combination with the 6-311++G(2d,2p) basis set are presented in the Table 5.

i. Influence of the functional on the QTAIM topological description of the free B-H bonds

A high electron density at the BCP, in combination with a negative $\nabla^2\rho$, is a signature of a covalent bond. Thus, a correct level of theory should lead to high ρ and negative $\nabla^2\rho$ at the BCP of the free B-H bonds ($BCP_{B\text{-}H\ free}$). The results reported in the Table 5 show that the electron density and the $\nabla^2\rho$ at the $BCP_{B\text{-}H\ free}$ are in the [0.169; 0.174], and [-0.159; -0.270] ranges, respectively. The covalent character of the free B-H bonds is thus well reproduced with all the selected functionals for the Ti^{+III}(1) compound, even if the Laplacian of the electron density is more sensitive to the choice of the functional than the electron density itself. More specifically, the M06-L local functional, the TPSSh hybrid functional, and the TPSSTPSS, TPSSTPSS-D3 meta-GGA functionals lead to smaller Laplacian of the electron density at the $BCP_{B\text{-}H\ free}$, relatively to the other functional.

ii. Influence of the functional on the QTAIM topological description of the agostic B-H bond

Compared with the free B-H bond, the agostic B-H bond is characterized by lower values of ρ and $\nabla^2\rho$ at the BCP. The difference between the mean values obtained for the free B-H bond and the agostic B-H bond will be denoted as $\Delta\rho = \rho(BCP_{B\text{-}H\ free}) - \rho(BCP_{B\text{-}H\ agostic})$ and $\Delta\nabla^2\rho = \nabla^2\rho(BCP_{B\text{-}H\ free}) - \nabla^2\rho(BCP_{B\text{-}H\ agostic})$, respectively. Using these definitions, $\rho(BCP_{B\text{-}H\ agostic})$ is calculated in the [0.122 ; 0.130] range, and Δ ρ is in the [0.047 ; 0.049] range, except in the case of calculations with the M06-L functional, for which Δ ρ is calculated to be Δ ρ= 0.039 a.u. $\nabla^2\rho(BCP_{B\text{-}H\ agostic})$ and $\Delta\nabla^2\rho$ are calculated in the [-0.051 ; 0.027] and [-0.249 ; -0.184] ranges, respectively.

As in the case of the free B-H bond, the value of the Laplacian of the electron density at the $BCP_{B\text{-}H\ agostic}$ is more sensitive to the choice of the functional than the value of the electron density itself. Furthermore, the Laplacian $\nabla^2\rho(BCP_{B\text{-}H\ agostic})$ is closed to zero, whatever the choice of the functional is. Using the M06-L local functional, the TPSSh hybrid functional, and the TPSSTPSS, TPSSTPSS-D3 meta-GGA functionals, weakly positive values are obtained, whereas the Laplacian is weakly negative where calculations are carried out with the other functionals. Furthermore, the total energy density is calculated to be in the [-0.117 ; -0.108] range.

This result demonstrates that the interaction of the B-H bond with the metallic centre leads to a weakening of the B-H bond.

	$BCP_{Ti\text{-}H\ agostic}$				$BCP_{B\text{-}H\ agostic}$				$BCP_{B\text{-}H\ free}$			$BCP_{Ti\text{-}N}$		
	ρ	$\nabla^2\rho$	ε	H	ρ	$\nabla^2\rho$	ε	H	ρ	$\nabla^2\rho$	ε	ρ	$\nabla^2\rho$	ε
B3LYP	0.057	0.150	0.436	-0.009	0.125	-0.014	0.149	-0.112	0.174	-0.259	0.044	0.068	0.229	0.293
B3LYP-D3	0.059	0.154	0.434	-0.009	0.126	-0.012	0.147	-0.113	0.174	-0.258	0.044	0.070	0.236	0.293
B3PW91	0.059	0.151	0.441	-0.010	0.123	-0.010	0.145	-0.110	0.171	-0.241	0.043	0.070	0.237	0.299
TPSSh	0.059	0.159	0.408	-0.009	0.122	0.017	0.147	-0.108	0.171	-0.208	0.039	0.069	0.237	0.279
TPSSTPSS	0.059	0.156	0.374	-0.009	0.122	0.003	0.147	-0.108	0.171	-0.218	0.037	0.068	0.230	0.260
TPSSTPSS-D3	0.060	0.159	0.372	-0.010	0.123	0.003	0.146	-0.108	0.171	-0.217	0.037	0.070	0.235	0.260
M06-L	0.055	0.162	0.430	-0.006	0.130	0.027	0.161	-0.117	0.169	-0.159	0.047	0.067	0.250	0.270
M06	0.058	0.154	0.429	-0.009	0.128	-0.024	0.133	-0.116	0.171	-0.226	0.044	0.071	0.247	0.269
BP86	0.059	0.143	0.373	-0.010	0.122	-0.051	0.143	-0.108	0.170	-0.270	0.038	0.068	0.221	0.260
BP86-D3	0.061	0.146	0.372	-0.010	0.123	-0.051	0.141	-0.109	0.170	-0.269	0.038	0.070	0.228	0.260
LC-ωPBE	0.060	0.157	0.517	-0.010	0.125	-0.004	0.131	-0.112	0.172	-0.253	0.048	0.073	0.248	0.334
LC-ωPBE-D3	0.061	0.160	0.516	-0.011	0.125	-0.004	0.130	-0.112	0.172	-0.253	0.048	0.073	0.252	0.334
PBE1PBE	0.060	0.153	0.464	-0.010	0.123	-0.004	0.142	-0.110	0.171	-0.235	0.043	0.123	-0.004	0.142
PBE1PBE-D3	0.060	0.155	0.463	-0.011	0.124	-0.004	0.141	-0.110	0.171	-0.234	0.043	0.072	0.248	0.308

Table 5: Effect of the functional on the QTAIM topological description of the protonated basin for the hydrogen atom involved in the agostic interaction with the metallic centre, in the Ti^{+III}(1) compound. All the calculations were carried out with the 6-311++G(2d,2p) basis set. All the values are given in atomic units.

iii. *Influence of the functional on the QTAIM topological description of the Ti-H interaction*

First of all, it is worth noticing that the agostic interaction is characterized by a BCP between the metallic centre and the agostic hydrogen atom, with all the selected functionals. The weak value of the electron density at the $BCP_{M\text{-}H\ agostic}$ ($\rho(BCP_{Ti\text{-}H\ agostic})$ is calculated in the [0.055 ; 0.061] range), together with the positive value of the Laplacian of the electron density ($\nabla^2\rho(BCP_{Ti\text{-}H\ agostic})$ is calculated in the [0.143 ; 0.162] range) and the very small value of the energy density (H is calculated in the [-0.011 ; -0.006] range), suggest that the agostic interaction is a closed-shell (non-covalent) interaction.

As expected for an agostic interaction, the ellipticity associated with the $BCP_{M\text{-}H\ agostic}$ is substantially larger than in the case of the B-H or M-N bonds.[67]

The results summed up in the Table 6 also demonstrate that all the selected functionals lead to consistent descriptions of the interaction. The B3LYP hybrid functional was selected for a further evaluation of the effect of the basis set on the QTAIM description of the Ti^{+III}(1) compound.

b. Influence of the basis set in combination with the B3LYP functional

The QTAIM topological characteristics of the M-H interaction, as well as the agostic B-H, free B-H and M-N bonds, obtained from calculations using each of the selected basis sets, are summed up in the Table 6.

i. *Influence of the basis set on the QTAIM topological description of the free B-H bonds*

When the B3LYP functional is used, the electron density and its Laplacian at the $BCP_{B\text{-}H\ free}$, are calculated to be in the range [0.160; 0.177] and [-0.051; -0.325], respectively. These values are consistent with the description of a covalent bond. Thus, as with the selected functionals combined with the 6-311++G(2d,2p) basis set, all the selected basis sets combined with the B3LYP hybrid functional lead to a consistent description of the free B-H bond.

ii. *Influence of the basis set on the QTAIM topological description of the agostic B-H bond*

Regardless of the basis set used, the B-H bond involved in the agostic interaction is characterized by $\rho(BCP_{B\text{-}H\ agostic})$ is calculated in the [0.118 ; 0.128] range, and $\nabla^2\rho(BCP_{B\text{-}H\ agostic})$ in the [-0.068 ; 0.097] range. The difference between the mean values obtained for the free B-H bond and the agostic B-H bond ($\Delta\rho = \rho(BCP_{B\text{-}H\ free}) - \rho(BCP_{B\text{-}H\ agostic})$ and $\Delta\nabla^2\rho = \nabla^2\rho(BCP_{B\text{-}H\ free}) - \nabla^2\rho(BCP_{B\text{-}H\ agostic})$) are in the ranges [0.042 ; 0.050] for $\Delta\rho$ and [-0.270 ; -0.148] for $\Delta\nabla^2\rho$. These values clearly underline the weakening of the B-H bond due to the agostic interaction. Furthermore, the B-H bond involved in the agostic interaction is also characterized by a total energy density of $H(BCP_{B\text{-}H\ agostic})$ in the [-0.125 ; -0.096] range. The weakly negative value of the energy density suggests that the agostic B-H bond is characterized by a weak covalent character.

iii. *Influence of the basis set on the QTAIM topological description of the Ti-H interaction*

A BCP was found between the metallic centre and the agostic hydrogen, with all the basis sets selected for the resent study. The electron density at the BCP is calculated to be weak, whatever the basis set used ($\rho(BCP_{Ti\text{-}H\ agostic})$ is calculated in the [0.056 ; 0.060] range), and the Laplacian of the electron density is calculated to be positive ($\nabla^2\rho(BCP_{Ti\text{-}H\ agostic})$ is calculated to be in the [0.135 ; 0.159] range). Furthermore, the energy density is calculated to be in the [-0.007; -0.013] range, which suggests that the agostic interaction corresponds to a weak polar shared interaction.

	$BCP_{Ti\text{-}H\ agostic}$				$BCP_{B\text{-}H\ agostic}$				$BCP_{B\text{-}H\ free}$			$BCP_{Ti\text{-}N}$		
	ρ	$\nabla^2\rho$	ε	H	ρ	$\nabla^2\rho$	ε	H	ρ	$\nabla^2\rho$	ε	ρ	$\nabla^2\rho$	ε
6-311++G(2d,2p)+LanL2DZ	0.059	0.154	0.482	-0.013	0.125	-0.006	0.162	-0.112	0.174	-0.259	0.044	0.068	0.240	0.301
6-311++ G(2d,2p)+SDD	0.058	0.135	0.457	-0.012	0.125	-0.007	0.158	-0.112	0.174	-0.260	0.045	0.070	0.217	0.302
6-311++G(2d,2p)	0.057	0.150	0.436	-0.009	0.125	-0.014	0.149	-0.112	0.174	-0.259	0.044	0.068	0.229	0.293
6-311++G(3df,3pd)	0.058	0.146	0.452	-0.010	0.127	-0.045	0.127	-0.117	0.176	-0.315	0.040	0.069	0.219	0.279
Def2-TZVP	0.056	0.157	0.426	-0.007	0.126	-0.011	0.158	-0.118	0.174	-0.257	0.049	0.068	0.230	0.279
Def2-TZVPP	0.057	0.157	0.440	-0.007	0.126	-0.014	0.147	-0.119	0.175	-0.253	0.045	0.068	0.229	0.278
Def2-QZVPP	0.058	0.138	0.435	-0.012	0.128	-0.068	0.123	-0.125	0.177	-0.325	0.041	0.069	0.220	0.285
DKH2/DZP-DKH (9v)	0.059	0.140	0.429	-0.013	0.118	0.074	0.149	-0.096	0.160	-0.080	0.055	0.070	0.224	0.303
RESC/DZP-DKH (9v)	0.059	0.140	0.429	-0.013	0.118	0.074	0.150	-0.096	0.160	-0.079	0.052	0.070	0.223	0.302
DKH2/TZP-DKH (9v)	0.058	0.156	0.436	-0.009	0.126	-0.045	0.138	-0.125	0.176	-0.287	0.046	0.069	0.225	0.280
DZP(9v)	0.058	0.138	0.433	-0.012	0.118	0.068	0.151	-0.096	0.160	-0.086	0.054	0.070	0.222	0.299
TZP(9v)	0.058	0.156	0.420	-0.009	0.126	-0.038	0.140	-0.125	0.176	-0.280	0.045	0.068	0.224	0.277
6-311++G(2d,2p)+LanL2DZ + single point with DKH2/DZP-DKH	0.060	0.145	0.420	-0.013	0.121	0.097	0.157	-0.098	0.164	-0.051	0.056	0.069	0.222	0.307

Table 6: Effect of the basis set on the QTAIM topological description of the protonated basin for the hydrogen atom involved in the agostic interaction with the metallic centre, in the Ti^{+III}(1) compound. All the calculations were carried out with the B3LYP functional. All the values are given in atomic units.

The results reported in the Tables 5 and 6 suggest that a single point calculation with the relativistic DKH2/DZP-DKH basis set, from a geometry optimized with the B3LYP functional, in combination with the LanL2DZ basis set for the metallic atom and the 6-311++G(2d,2p) basis set for all the other atoms, leads to a consistent QTAIM topological description of β B-H agostic interactions, in the case of the family of compounds herein considered. This is the reason why the following methodology was selected:

1. First of all, the geometry of the compounds were built up from the information available from the literature, and fully optimized with the B3LYP functional, in combination with the LanL2DZ basis set for the metallic atom and the 6-311++G(2d,2p) basis set for all the other,
2. Then, a single point calculation was carried out using the DKH2 Hamiltonian in combination with the B3LYP/DZP-DKH level of theory,
3. The ELF method was further used to ascertain the presence of a trisynaptic, agostic, protonated basin,
4. Finally, the M-H interaction and the agostic B-H bond were further probed and characterized thanks to their signatures within the QTAIM framework, in terms of the electron density ρ, the Laplacian of the electron density $\nabla^2\rho$, the ellipticity ε, and the total energy density H, at the BCP's.

c. Influence of the nature of the substituents and the metallic centre

To further understand the impact of the nature of the metal and of the ligand on the agostic character of a σ(B-H) bond in β position, additional compounds were considered and finally 54 complexes were selected for the present study (Figure 1). We would like to underline the fact that, beyond the nine experimentally identified complexes, the existence of 45 the other structures involving a β agostic interaction has yet to be demonstrated.

To begin with, it is interesting to compare the geometries calculated at the B3LYP/6-311++G(2d,2p)+ LanL2DZ level of theory for the 54 considered species. The Cartesian coordinates are given in Supporting Information. A general feature concerns the relative positions of the M,X,B and agostic H atoms : in the case of the compounds M(1), M(2), M(4), M(5),and M(6) species, these four atoms are coplanar. The M(3) species appear as an exception to this geometrical property. Indeed, for the Ti_z^{+IV}(3), Zr^{+III}(3), Hf^{+III}(3), Zr_z^{+IV}(3) , Hf_z^{+IV}(3) and Zr_e^{+IV}(3) species, a geometric distortion occurs and the four atoms are no more coplanar.

The mono-agostic compounds were further characterized by means of the ELF and QTAIM topological approaches. The ELF analysis systematically confirms the presence of a trisynaptic basin for the agostic hydrogen atom, with a population close to 2 electrons, and with a non-negligible contribution of the metallic centre (Table S4). Finally, the strength of the β B-H agostic interaction in each species was quantitatively characterized by means of the QTAIM topological approach (Table S5). For all the considered compounds, a BCP between the M and H atoms ($BCP_{M\text{-}H\ agostic}$) further confirms the existence of a β B-H agostic interaction. Within a same family of compounds, a stronger interaction will be characterized by a higher electron density at the $BCP_{M\text{-}H\ agostic}$, and a shorter $M\text{-}H_{agostic}$ distance. Thus, for a better comparison of the strength of the interaction, in each compound, the $M\text{-}H_{agostic}$ distance was plotted as a function of the $\rho(BCP_{M\text{-}H\ agostic})$ (Figure 2).

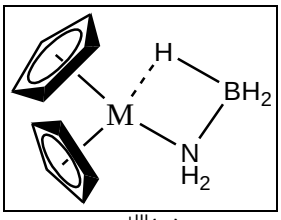

M^{+III}(1)

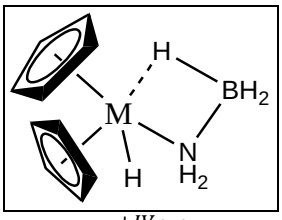

M_e^{+IV}(1)

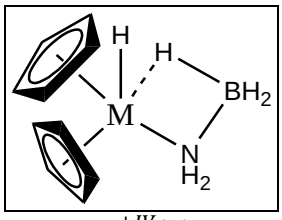

M_z^{+IV}(1)

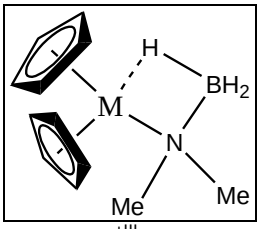

M^{+III}(2)

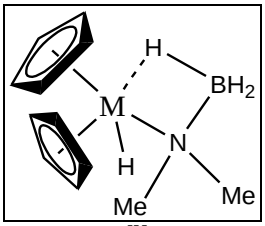

M_e^{+IV}(2)

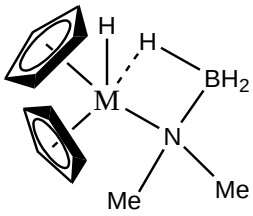

M_z^{+IV}(2)

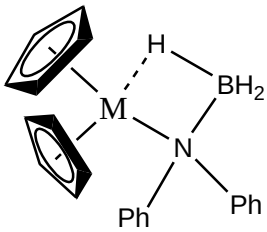

M^{+III}(3)

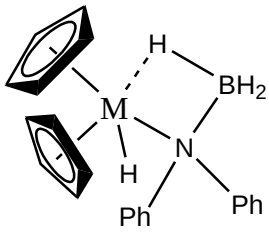

M_e^{+IV}(3)

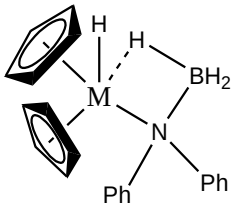

M_z^{+IV}(3)

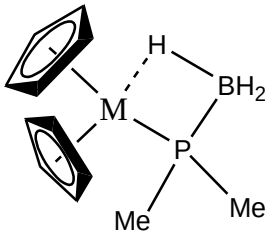

M^{+III}(4)

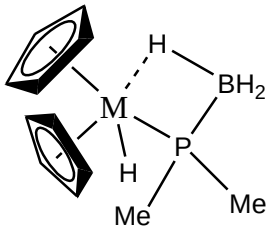

M_e^{+IV}(4)

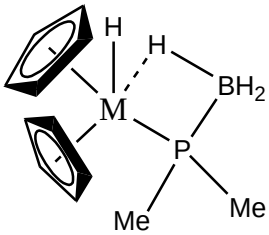

M_z^{+IV}(4)

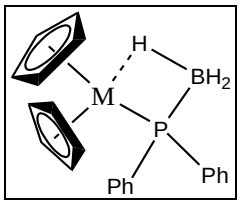

M^{+III}(5)

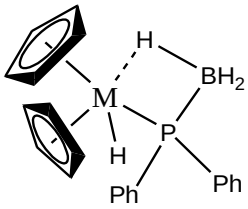

M_e^{+IV}(5)

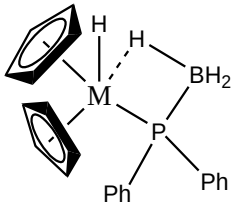

M_z^{+IV}(5)

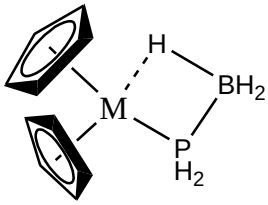

M^{+III}(6)

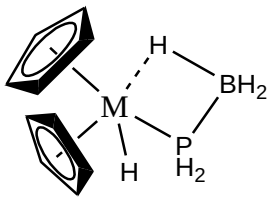

M_e^{+IV}(6)

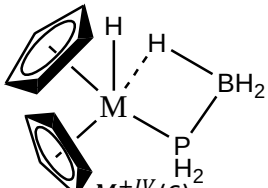

M_z^{+IV}(6)

Figure 1: Group 4 metallocene compounds involving an agostic interaction with a σ(B-H) bond in β position that were considered for the present study. The compounds for which experimental data are available are presented in a frame.

In order to evaluate both the influence of the borane ligand and the metallic centre, two graphs were built up with the same data. The variation of the M-H $_{agostic}$ distance as a function of the ρ($BCP_{M\text{-}H\ agostic}$) is shown for each borane ligands in the Figure 2A, and for each of the metallic centre in the Figure 2B.

The figure 2A clearly suggests that the β B-H agostic interaction is systematically stronger with amine-boranes compared to phosphine-boranes. The comparison of the agostic character of the species depending on the nature of the metallic centre (Figure 2B) clearly suggests that the agostic interaction is stronger in the titanocene compounds compared with the zirconocene and hafnocene species.[68] Furthermore, the agostic interaction in the paramagnetic titanium species may be as strong as in diamagnetic species.

It is interesting to compare these theoretical results with experimental observations, based on the study of the whole dehydrogenation process (global turn-over of the reaction, identification of the products, and structural characterization of intermediates). The experimental results have unveiled several features of the amine-borane dehydrogenation:

- In a study centered on Rh-containing organometallic catalysts, Manners et al. have demonstrated that dehydrogenation reaction proceeds more efficiently amine-boranes compared to phosphine-borane, [69]
- The turnovers of the dehydrogenation reactions with titanocene catalysts are often reported to be bigger compared to the ones obtained with zirconocenes and hafnocenes,[68, 70]
- The study of the dehydrogenation reaction using a metallocene catalyst involving a paramagnetic metallic centre has proven that such centres can be as efficient as diamagnetic species. [25]

The close agreement between the calculated strength of the agostic bond and the experimental efficiency of the dehydrogenation processes may suggest that the agostic intermediate might have a prominent role in the reaction mechanism.

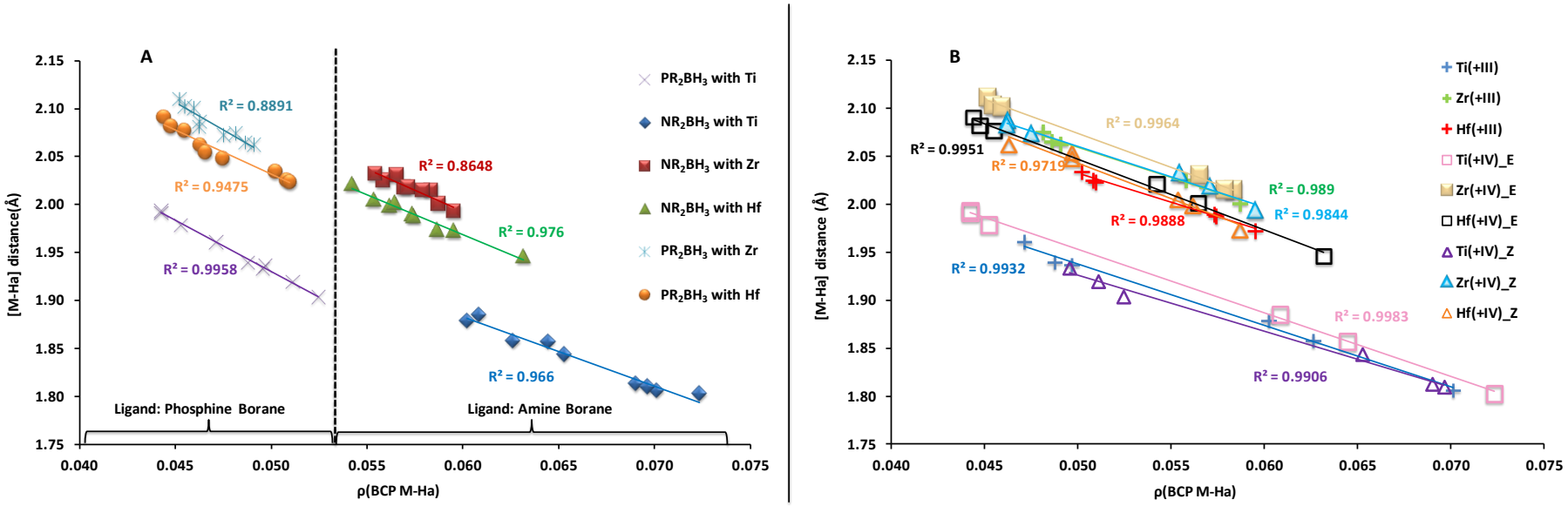

Figure 2: Variation of the M-H $_{agostic}$ distance as a function of the ρ(BCP$_{M\text{-}H\ agostic}$): A : for each borane ligands presented in the Figure 1; B: for each of the metallic centre (i.e. paramagnetic Ti, Zr and Hf, or diamagnetic (Z or E) Ti, Zr and Hf).

Conclusion

The aim of the present work was to evaluate the influence of different parameters on the strength of an agostic B-H interaction. A calibration study based on the $Cp_2TiNH_2BH_3$ titanocene compound was carried out to estimate the ability of several DFT levels of theories to reproduce geometric and topological properties of the agostic interaction involved in this compound. We were particularly interested in identifying the smallest level of theory leading to a consistent description of the system. A comparison with experimental (crystallographic) data has shown that the B3LYP/6-311++G(2d,2p)+LanL2DZ level of theory leads to an accurate description of the system from a geometric point of view. Further topological characterizations using the electron localization function at the same level of theory leads to an underestimation of the contribution of the metallic centre in the agostic protonated basin. Thus, a whole-electron basis set should be used for an accurate ELF characterization of the agostic interaction. For a comparative study of titanocenes, zirconocenes and hafnocenes, we thus recommend the use of the DKH relativistic Hamiltonian, in combination with the DZP-DKH basis set. In order to save computational time, a single point relativistic calculation can be carried out from a geometry optimized at the B3LYP/6-311++G(2d,2p)+LanL2DZ level of theory.

Using the B3LYP/DZP-DKH//(B3LYP/6-311++G(2d,2p)+LanL2DZ level of theory, 54 compounds of the group 4 metallocenes, involving differently substituted amine- and phosphine-boranes, were studied. In the case of the Ti_z^{+IV}(3) compound, the optimized structure does not correspond to a mono-agostic, but to a bi-agostic species. For all the other species considered, a mono-agostic interaction was confirmed by the topological analysis. Indeed, a trisynaptic protonated basin involving ~ 2 electrons with a non-negligible contribution of the metallic centre was identified thanks to the ELF analysis. This is the signature of a 3C/2e interaction. Furthermore, using the QTAIM approach, a BCP was identified between the agostic hydrogen atom and the metallic centre in each of the compounds. The properties of this $BCP_{M\text{-}H\ agostic}$ (the electron density ρ, the Laplacian of the electron density $\nabla^2\rho$, the ellipticity ε, and the total energy density H) were then used to further characterize the interaction.

General trends emerge from this study of the influence of the nature of the metallic centre and the substitution of amine- and phosphine-boranes on the strength of the agostic interaction. Stronger interactions were identified in the case of amine-boranes compared with phosphine-boranes. As far as the metallic centre is concerned, stronger interactions were identified in the case of titanocenes compared with zirconocenes and hafnocenes. The agostic interactions in paramagnetic compounds can be as strong as in the case of the diamagnetic compounds.

The present study demonstrates the feasibility of a comparative study of B-H agostic interactions in a wide set of compounds, including first-, second-, and third-row metallic centres. The use of DFT calculations in combination with the ELF and QTAIM approaches allows the characterization of the 3C/2e interaction. This work constitutes a first step toward a comprehensive study of the whole reaction mechanisms involved in the dehydrogenation processes of boranes.

---

[1] Johnson HC, Hooper TN, Weller AS (2015) The Catalytic Dehydrocoupling of Amine–Boranes and Phosphine–Boranes. Top Organomet Chem. 49: 153-220

[2] Staubitz A, Robertson APM, Sloan ME, Manners I (2010) Amine- and Phosphine-Borane Adducts: New Interest in Old Molecules. Chem Rev 110: 4023–4078

[3] Alcaraz G, Sabo-Etienne G (2010) Coordination and Dehydrogenation of Amine–Boranes at Metal Centers. Angew Chem Int Ed 49: 7170–7179

[4] Whittell GR, Manners I (2011) Advances with Ammonia-Borane: Improved Recycling. Angew Chem Int Ed 50: 10288–10289
[5] Leitao EM, Jurca T, Manners I (2013) Catalysis in service of main group chemistry offers a versatile approach to p-block molecules and materials. Nature Chemistry 5: 817-829
[6] Waterman R (2013) Mechanisms of metal-catalyzed dehydrocoupling reactions. Chem Soc Rev 42: 5629-5641
[7] Rossin A, Peruzzini M (2016) Ammonia − Borane and Amine − Borane Dehydrogenation Mediated by Complex Metal Hydrides. Chem Rev ASAP Article, DOI : 10.1021/acs.chemrev.6b00043
[8] Kubas GJ (2007) Dihydrogen complexes as prototypes for the coordination chemistry of saturated molecules. PNAS 1047: 6901-6907
[9] Brookhart M, Green MHL, Parkin G (2007) Agostic interactions in transition metal compounds. PNAS 104: 6908-6914
[10] Clots E, Eisenstein O (2004) Agostic Interactions from a Computational Perspective: One Name, Many Interpretations. Struct Bond 113: 1-36
[11] Brookhart M, Green MLH, Pardy RBA (1983) Two-electron,three-centre carbon–hydrogen–cobalt bonds in the compounds [Co(Z-C_5Me_4R)(Z-C_2H_4)(Z-C_2H_4-m-H)]BF_4,R = Me and Et. J Chem Soc Chem Commun 691–693
[12] Brookhart M, Green MLH (1983) Carbon-hydrogen-transition metal bonds. J Organomet Chem 250: 395–408
[13] Becke AD, Edgecombe KE (1990) A simple measure of electron localization in atomic and molecular systems. J Chem Phys 92: 5397-5403
[14] Bader RFW (1990) Atoms in Molecules-A Quantum Theory, Oxford University Press, Oxford. ISBN: 0198558651
[15] Matta CF, Boyd RJ (2007) An Introduction to the Quantum Theory of Atoms in Molecules. In The Quantum Theory of Atoms in Molecules. Matta and Boyd (Editor)
[16] von Frantzius G, Streubel R, Brandhorst K, Grunenberg J (2006) How Strong Is an Agostic Bond? Direct Assessment of Agostic Interactions Using the Generalized Compliance Matrix. Organometallics 25 : 118-121
[17] Pantazis DA, McGrady JE, Maseras F, Etienne M (2007) Critical Role of the Correlation Functional in DFT Descriptions of an Agostic Niobium Complex. J Chem Theory Comput 4: 1329-1336
[18] Lein M (2009) Characterization of agostic interactions in theory and computation. Coord Chem Rev 253: 625-634
[19] Grimme S, Steinmetz M (2013) Effects of London dispersion correction in density. Phys Chem Chem Phys 15: 16031-16042
[20] Eickerling G, Mastalerz R, Herz V, Scherer W, Himmel H J, Reiher M (2007) Relativistic effects on the topology of the electron density. J Chem Theory Comput 3*:* 2182-2197.
[21] Bučinský L, Kucková L, Malček M, Kožíšek J, Biskupič S, Jayatilaka D, Büchel GE, Arion VB (2014) Picture change error in quasirelativistic electron/spin density, Laplacian and bond critical points. J Chem Phys 438: 37-47
[22] Bučinský L, Jayatilaka D, Grabowsky S (2016) Importance of Relativistic Effects and Electron Correlation in Structure Factors and Electron Density of Diphenyl Mercury and Triphenyl Bismuth. J Phys Chem A 120: 6650-6669
[23] Wolstenholme DJ, Traboulsee KT, Decken A, McGrady CS (2009) Structure and bonding of titanocene amidoborane complexes: a common bonding motif with their β-agostic organometallic counterparts. Organometallics 29: 5769-5772
[24] Forster TD, Tuononen HM, Parvez M, Roesler R (2009) Characterization of β-Agostic isomers in Zirconocene Amidoborane complexes. J Am Chem Soc 131: 6689–6691
[25] Helten H, Dutta B, Vance JR, Sloan ME, Haddow MF, Sproules S, Collison D, Whittell GR, Lloyd-Jones GC, Manners I (2013) Paramagnetic titanium(III) and zirconium(III) metallocene complexes as precatalysts for the dehydrocoupling/dehydrogenation of amine-borane. Angew Chem Int Ed 52: 437-440
[26] Gaussian 09, Revision E.01, Frisch MJ, Trucks GW, Schlegel HB, Scuseria GE, Robb MA, Cheeseman JR, Scalmani G, Barone V, Mennucci B, Petersson GA, Nakatsuji H, Caricato M, Li X, Hratchian HP, Izmaylov AF, Bloino J, Zheng G, Sonnenberg JL, Hada M, Ehara M, Toyota K, Fukuda R, Hasegawa J, Ishida M, Nakajima T, Honda Y, Kitao O, Nakai H, Vreven T, Montgomery JA, Peralta JE, Ogliaro F, Bearpark M, Heyd JJ, Brothers E, Kudin KN, Staroverov VN, Kobayashi R, Normand J, Raghavachari K, Rendell A, Burant JC, Iyengar SS, Tomasi J, Cossi M, Rega N, Millam JM, Klene M, Knox JE, Cross JB, Bakken V, Adamo C, Jaramillo J, Gomperts R, Stratmann RE, Yazyev O,Austin AJ, Cammi R, Pomelli C, Ochterski JW, Martin RL, Morokuma K, Zakrzewski VG, Voth GA,

Salvador P, Dannenberg JJ, Dapprich S, Daniels AD, Farkas Ö, Foresman JB, Ortiz JV, Cioslowski J, Fox DJ (2009) Gaussian, Inc, Wallingford CT
[27] Zhao Y, Truhlar DG (2011) Applications and validations of the Minnesota density functionals. Cheml Phys Lett 502: 1-13
[28] Toulouse J, Savin A, Flad HJ (2004) Short-Range Exchange-Correlation Energy of a Uniform Electron Gas with Modified Electron–Electron Interaction. Int J Quantum Chem 100: 1047–1056
[29] Goerigk L (2015) Treating London-Dispersion Effects with the Latest Minnesota Density Functionals: Problems and Possible Solutions. J Phys Chem Lett 6: 3891–3896
[30] Zhao Y, Truhlar GD (2008) The M06 suite of density functionals for main group thermochemistry, thermochemical kinetics, noncovalent interactions, excited states, and transition elements: two new functionals and systematic testing of four M06-class functionals and 12 other functionals. Theor Chem Acc 120: 215–241
[31] Modrzejewski M, Chalasinski G, Szczęsniak MM (2014) Range-Separated meta-GGA Functional Designed for Noncovalent Interactions. J Chem Theory Comput 10: 4297 − 4306
[32] Grimme G (2011) Density functional theory with London dispersion corrections. WIREs Comput Mol Sci 1: 211–228
[33] Grimme S, Antony J, Ehrlich S, Krieg H (2010) A consistent and accurate ab initio parametrization of density functional dispersion correction (DFT-D) for the 94 elements H-Pu. J Chem Phys 2010 132: 154104
[34] Xing YM, Zhang L, Fang DC (2015) DFT Studies on the Mechanism of Palladium(IV)-Mediated C–H Activation Reactions: Oxidant Effect and Regioselectivity. Organometallics 34: 770–777
[35] van der Eide EF, Yang P, Bullock RM (2013) Isolation of two agostic isomers of an organometallic cation: different structures and colors. Angew Chem 125: 10380–10384
[36] Zhao Y, Truhlar DG (2006) A new local density functional for main-group thermochemistry, transition metal bonding, thermochemical kinetics, and noncovalent interactions. J Chem Phys 125: 194101
[37] Perdew PJ (1986) Density-functional approximation for the correlation energy of the inhomogeneous electron gas. Phys Rev B 34: 7406
[38] Staroverov NV, Scuseria GE, Tao JM, Perdew JP (2003) Comparative assessment of a new nonempirical density functional: Molecules and hydrogen-bonded complexes. J Chem Phys 119: 12129
[39] Becke AD (1988) Density-functional exchange-energy approximation with correct asymptotic behavior. Phys Rev A 38: 3098–3100
Lee C, Yang W, Parr RG (1988) Development of the Colle-Salvetti correlation-energy formula into a functional of the electron density. Phys Rev B 37: 785–789
[40] Lee C, Yang WT, Parr RG (1988) Development of the Colle-Salvetti correlation-energy formula into a functional of the electron density. Phys Rev B: 785–789
[41] Perdew JP, Burke K, Ernzerhof M (1996) Generalized gradient approximation made simple. Phy Rev Lett 77: 3865-3868
[42] Perdew JP, Burke K, Ernzerhof M (1997) Errata: Generalized gradient approximation made simple. Phys Rev Lett 78: 1396
[43] Adamo C, Barone V (1999) Toward reliable density functional methods without adjustable parameters: The PBE0 model. J Chem Phys 110: 6158-6169
[44] Tao JM, Perdew JP, Staroverov VN, Scuseria GE (2003) Climbing the density functional ladder: Nonempirical meta-generalized gradient approximation designed for molecules and solids. Phys Rev Lett 91: 146401
[45] Vydrov OA, Scuseria GE (2006) Assessment of a long range corrected hybrid functional. J Chem Phys 125: 234109
[46] Vydrov OA, Heyd J, Krukau A, Scuseria GE (2006) Importance of short-range versus long-range Hartree-Fock exchange for the performance of hybrid density functionals. J Chem Phys 125: 074106
[47] Vydrov OA, Scuseria GE, Perdew JP (2007) Tests of functionals for systems with fractional electron number. J Chem Phys 126: 154109
[48] Neto AC, Muniz EP, Centoducatte R, Jorge FE (2005) Gaussian basis sets for correlated wave functions, Hydrogen, helium, first- and second-row atoms. J Mol Struct 718: 219-224
[49] Camiletti GG, Machado SF, Jorge FE (2008) Gaussian Basis Set of Double Zeta Quality for Atoms K Through Kr: Application in DFT Calculations of Molecular Properties. J Comp Chem 29: 2434-2444

[50] Barros CL, de Oliveira PJP, Jorge FE, Canal Neto A, Campos M (2010) Gaussian basis set of double zeta quality for atoms Rb through Xe: application in non-relativistic and relativistic calculations of atomic and molecular properties. Mol Phys 108: 1965-1972
[51] Barbieri PL, Fantin PA, Jorge FE (2006) Gaussian basis sets of triple and quadruple zeta valence quality for correlated wave functions. Mol Phys 104: 2945-2954
[52] Machado SF, Camiletti GG, Canal Neto A, Jorge FE, Jorge RS (2009) Gaussian basis set of triple zeta valence quality for the atoms from K to Kr: Application in DFT and CCSD(T) calculations of molecular properties. Mol Phys 107: 1713-1727
[53] Campos CT, Jorge EF (2013) Triple zeta quality basis sets for atoms Rb through Xe: application in CCSD(T) atomic and molecular property calculations. Mol Phys 111: 167-173
[54] Jorge EF, Canal Neto A, Camiletti GG, Machado SF (2009) Contracted Gaussian basis sets for Douglas-Kroll-Hess calculations: Estimating scalar relativistic effects of some atomic and molecular properties. J Chem Phys 130: 064108
[55] Canal Neto A, Jorge EF (2013) All-electron double zeta basis sets for the most fifth-row atoms: Application in DFT spectroscopic constant calculations. Chem Phys Lett 582: 158-162
[56] Barros CL, de Oliveira PJP, Jorge FE, Canal Neto A, Campos M (2010) Gaussian basis set of double zeta quality for atoms Rb through Xe: application in non-relativistic and relativistic calculations of atomic and molecular properties Gaussian basis set of double zeta quality for atoms Rb through Xe: application in non-relativistic and relativistic calculations of atomic and molecular properties. Mol Phys 108: 1965-1972
[57] Jorge FE, Canal Neto A, Camiletti GG, Machado SF (2009) Contracted Gaussian basis sets for Douglas-Kroll-Hess calculations: Estimating scalar relativistic effects of some atomic and molecular properties. J Chem Phys 130: 064108
[58] Ponec R, Bučinský L, Gatti C (2010) Relativistic Effects on Metal− Metal Bonding: Comparison of the Performance of ECP and Scalar DKH Description on the Picture of Metal− Metal Bonding in $Re_2Cl_8^{2-}$. J Chem Theory Comput 6: 3113-3121
[59] Savin A, Becke AD, Flad J, Nesper R, Preuss H, von Schnering HG (1991) Angew Chern Inr Ed Engl 30: 409-412
[60] Fuentealba P, Chamorro E, Santos JC (2007) Understanding and using the electron localization function. In Theoretical Aspects of Chemical Reactivity. Toro-Labbé (Editor). Published by Elsevier B.V.
[61] Tognetti V, Joubert L, Cortona P, Adamo C (2009) Toward a Combined DFT/QTAIM Description of Agostic Bonds: The Critical Case of a Nb(III) Complex. J Phys Chem A 113 : 12322-12327
[62] Tognetti V, Joubert L, Raucoules R, de Bruin T, Adamo C (2012) Characterizing Agosticity Using the Quantum Theory of Atoms in Molecules: Bond Critical Points and Their Local Properties. J Phys Chem A 116: 5472−5479
[63] Tognetti V, Joubert L (2011) On the Influence of Density Functional Approximations on Some Local Bader's Atoms-in-Molecules Properties. J Phys Chem A 115: 5505-5515
[64] Noury S, Krokidis X, Fuster F, Silvi B (1999) Computational tools for the electron localization function topological analysis. Comput Chem 23: 597–604
[65] Keith TA, AIMAll (Version 14.10.27), TK Gristmill Software, Overland Park KS, USA, 2014 (aim.tkgristmill.com)
[66] Zins EL, Silvi B, Alikhani ME (2015) Activation of C-H and B-H bonds through agostic bonding: an ELF/QTAIM insight. Phys Chem Chem Phys 27: 9258-9281
[67] Jablonski M (2015) QTAIM-Based Comparison of Agostic Bonds and Intramolecular Charge-Inverted Hydrogen Bonds. J Phys Chem A: 119, 4993–5008
[68] Pun D, Lobkovsky E, Chirik PJ (2007) Amineborane dehydrogenation promoted by isolable zirconium sandwich, titanium sandwich and N_2 complexes. Chem Commun 31: 3297-3299
[69] Jaska CA, Manners I (2004) Heterogeneous or Homogeneous Catalysis, Mechanistic Studies of the Rhodium-Catalyzed Dehydrocoupling of Amine-Borane and Phosphine-Borane Adducts. J Am Chem Soc 126: 9776–9785
[70] Sloan ME, Staubitz A, Clark TJ, Russell CA, Lloyd-Jones GC, Manners I (2010) Homogeneous Catalytic Dehydrocoupling/Dehydrogenation of Amine-Borane Adducts by Early Transition Metal, Group 4 Metallocene Complexes. J Am Chem Soc 132: 3831–3841